UNDERSTANDING THE ROLE OF MASK AND RESIST IN LINE-END SHORTENING WITH SIMULATION

by

Ivan Lee

Memorandum No. UCB/ERL M97/51

21 July 1997

UNDERSTANDING THE ROLE OF MASK AND RESIST IN LINE-END SHORTENING WITH SIMULATION

by

Ivan Lee

Memorandum No. UCB/ERL M97/51

21 July 1997

ELECTRONICS RESEARCH LABORATORY

College of Engineering
University of California, Berkeley
94720

Title: Understanding the Role of Mask and Resist in Line-End Shortening with Simulation

I. Introduction

Optical projection printing produces features that deviate from desired dimensions. For example, although mask patterns have square line-ends, the developed features usually have rounded corners and are typically shorter in length than on the mask. A contact is usually imaged by a square mask pattern, but the developed contact is nearly round. These nonidealities are caused by factors of optical imaging and factors of resist development.

Adjusting the process to fix one problem such as line-end shortening has detrimental effects on other issues like contact development. This is because the features have considerably different images. For a resist line in positive tone resist, the intensity of the imaged line increases gradually to its maximum value at the line-end because nonidealitiies prevent an abrupt change. The intensity of the contact is brightest near the contact's center but decreases gradually because of nonidealities of the image. A process that improves end-shortening by slowing the rate of development might adversely prevent a contact from completely opening. Finding the optimal conditions becomes a complex task because of the dissimilarity of the images for different features.

The goal of this project is to simulate both the optical effects of projection printing and resist characteristics of development to find methods to reduce line-end shortening. This is done by examining the difference between ideal mask sizes and developed patterns of line lengths, line widths, and contact size under different photolithographic conditions. The data generated helps the fabrication designer choose process parameters that will yield developed features within specified tolerances.

In this work, the TMA workbench [1] is used with Berkeley simulators to evaluate the response of the different lithographic features to three lithographic properties. Aerial imaging is simulated with SPLAT 5.0 [2], and resist dissolution simulation is performed with SAMPLE 1.8b [3]. By simultaneously varying the mask size, dose, and n - the contrast of the Mack resist, the workbench extracts line-end bias (ΔL), line width (ΔW), and contact size (ΔC) deviations from SAMPLE. The response data is then collected in a spreadsheet from which a response surface analysis is performed to locate empirical process conditions that will minimize the three outputs.

II. Line-end Shortening Problem

As the critical dimension of lithographic processes becomes smaller, issues of accuracy become ever more important. The amount of line-end shortening that was once tolerated contributes more to relative line length differences, and thereby affects the electrical properties of the integrated circuit. The photolithographic process must be examined to understand how end-shortening occurs.

The development of the resist involves optical imaging and chemical dissolution. When a positive resist is exposed, a light-induced chemical reaction produces acid in the resist. The acid regions are chemically removed by developing the resist with a base. The process engineer desires developed lines of the correct size and a wall-angle that approaches 90 degrees.

The optical properties for different features are apparent in the different mask images. Along the length of a line, the image intensity brightens to the clear field value after the line-end, which means that the resist at the end of the line may be attacked laterally from highly exposed regions on three sides. On the other hand, the image of the contact is brightest at the contact's center, which means the contact is formed by the *removal* of resist. To make contacts as small as possible, the peak brightness in the contact can be well below the clear field value. This difference in the image of these features suggests that an improvement in line formation could be detrimental to contact openings.

Another optical effect is the standing-wave patterns that appear in the exposed resist. At the time of exposure, light reflects at the interface between the resist and the substrate. The reflection produces a standing-wave pattern that can be seen in the developed side-wall. Instead of having a side-wall of constant slope, the resist has a rippled wall. The ripples and the slope of the side-wall affect the line length, which is often depicted by the swing curve [4]. To reduce the amplitude of these ripples, a heat-diffusion step can be incorporated between exposure and chemical development. The heat-diffusion spreads the acid more evenly at the boundary of exposure and yields a smoother side-wall upon development.

The optical system may not always be perfectly focused on the plane of the resist. If defocus exists, the maximum image intensity decreases at a line mask-edge and at the contact center. Furthermore, the low intensities in the middle of small opaque features also increase (Figure 1). In the case of the line, this increase may produce a shorter resist line. For the contact, the diminished peak intensity may not be enough to form a sufficiently-sized opening (Figure 2).

Thu May 22 16:03:13 1997

Figure 1:

Line Image - Mask Edge @ 1.0u - Mask Line-Width 0.5u

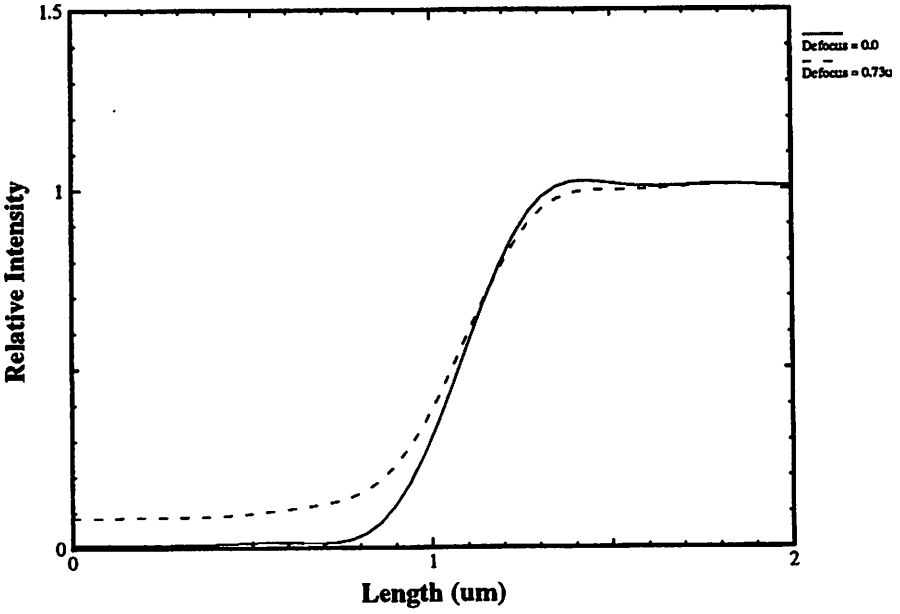

Thu May 22 16:03:43 1997

Figure 2:

Contact Image - Mask Edges @ .7u and 1.3u - Mask Contact-Width 0.6u

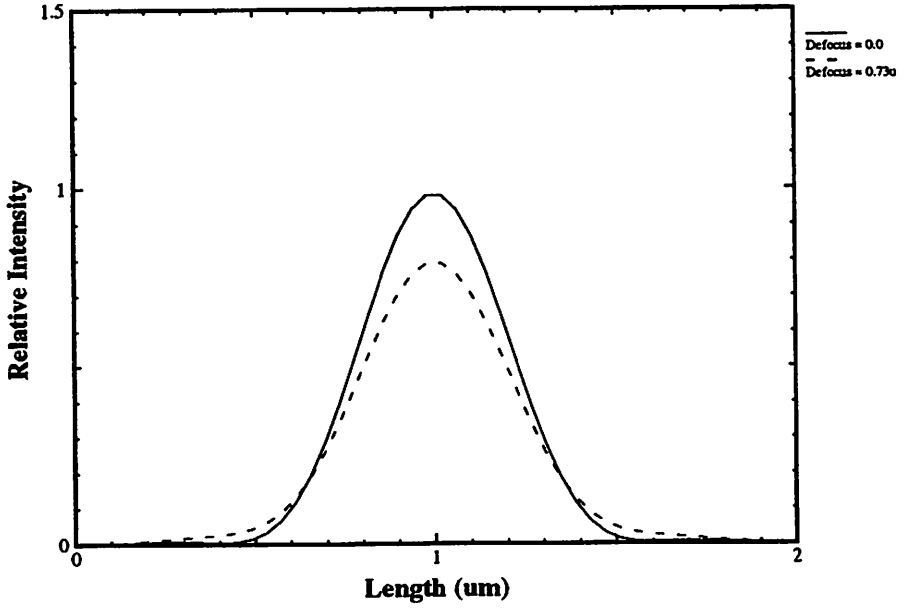

The dissolution characteristics of the photoresist also play a role and possibly provide compensation for the nonidealities of the image. The mask has features that would ideally be an abrupt pattern changing from maximum image intensity to zero intensity, but the square wave intensity is not achieved because the lens degrades the pattern to a sinusoid (again Figure 1). The role of the resist is to yield a line of specified length with a nearly perpendicular side-wall. This should be accomplished although the image intensity does not change abruptly at the mask-edge. Such a resist would need a rate which increased rapidly and nonlinearly with exposure dose.

The resist development rate is usually characterized as a function of M, which is the fraction of inhibitor remaining in the resist; the larger the M, the slower the development rate. The resist should not develop under low exposure doses, but above a certain dose threshold, maximum development rate would be desirable. In practice, the resist has a range of M values where a transition from minimum rate to maximum rate occurs (Figure 3).

Because the development rate does *not* change abruptly as a function of M for a resist, the top portions of resist may be shorter than regions near the resist-substrate interface. To reduce this top-loss, surface rate-retardation (or depth-dependent rate increase) could be added.

There are many resist models that can be used to optimize the lithographic process for line-end shortening. The Kim model [5] allows the incorporation of surface rate-retardation; the Hirai model [6] permits a selection of rate over the range of M; and the Mack model [7] generates a development rate with a transition between minimum and maximum rate over a small range of M. The rate vs. M curves are shown in Figure 3.

An interesting and illustrative example is the effect of the n parameter in the Mack model. The Mack equation is shown below with the standard values of the equation parameters used in this study shown in Table 1.

$$rate_{Mack} = R_{max}\frac{(a+1)\,(1-M)^{n}}{a+\,(1-M)^{n}} + R_{min}$$

Thu May 22 18:53:44 1997

Figure 3:
Model Rate Curves

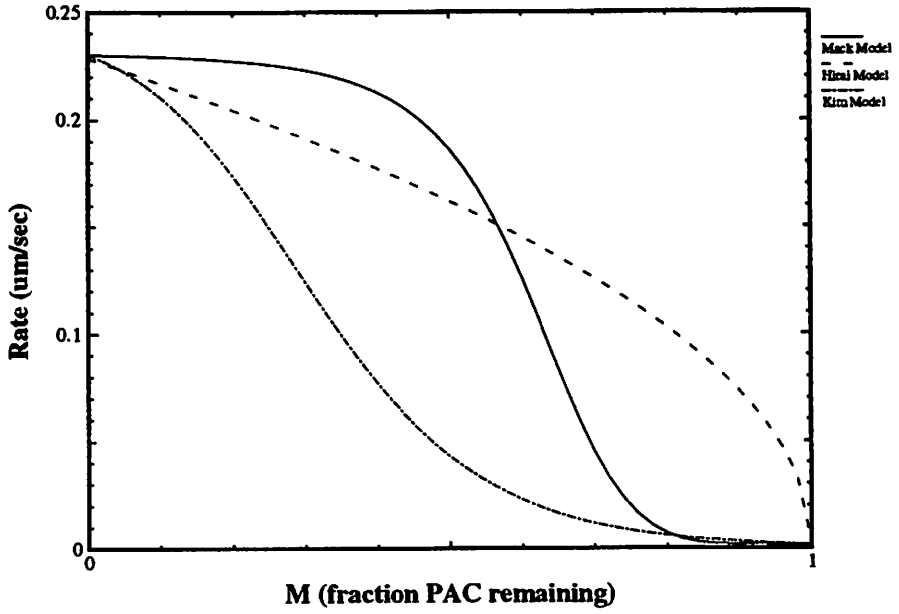

Table 1: Mack Model Standard Values

Mack Parameter	Value
Rmax	0.2284 um/sec
Rmin	0.0016 um/sec
a	0.005
n	5.6

In Figure 4 the rate curves have a higher dose threshold as n is increased. The amount of photoactive compound remaining decreases upon exposure; thus the lower M values yield faster development rates. The s-shaped curves of the Mack model are particularly good models of resists that can tolerate some amount of exposure without significant development. The s-shape is indicative of high contrast resists and is helpful in preventing defocus from causing excessive end-shortening. As n is increased, the resist should be more tolerant of low exposure doses, but contacts imaged on the same mask may be more difficult to develop. Thus the n value in the Mack model is an interesting parameter to examine in finding optimal resist properties for reducing line-end shortening.

Figure 4:

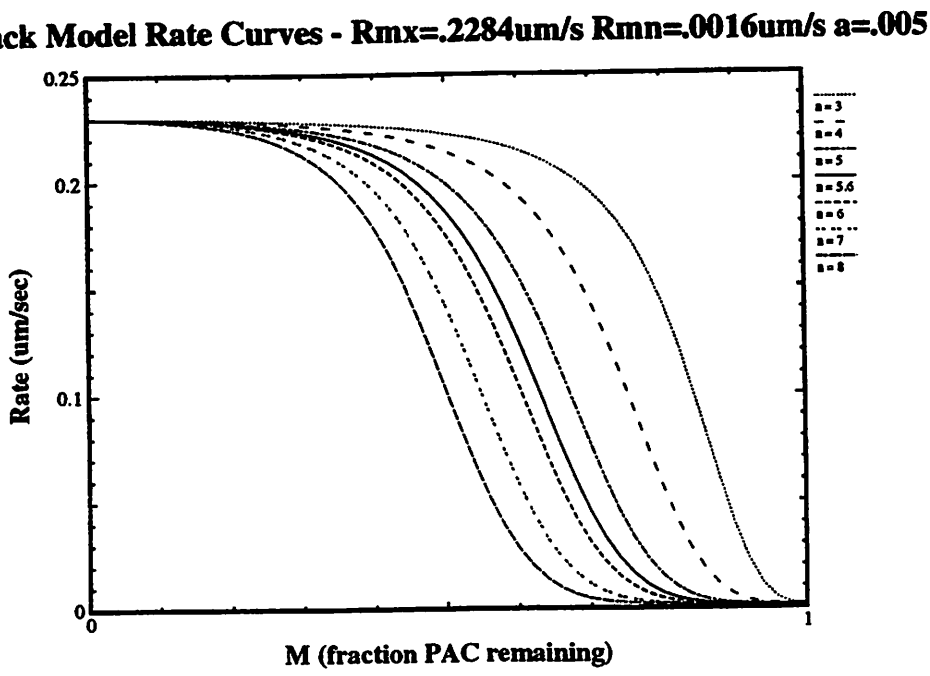

In review, the optical system of a photolithographic process has nonideal behaviors which include standing-wave patterns and defocus that affect the images of lines and contacts differently. The proposed solution for these nonidealities is to choose a resist that is insensitive to defocus and produces accurate feature sizes. Consider for example the difference between line and contact. By making line lengths and line widths more accurate by choosing a more defocus tolerant resist, contacts imaged on the same mask may be smaller than desired. The goal of this study is to find a set of process conditions that reduces end-shortening while also producing lines and contacts of sizes within constraints.

III. Simulation Methodology

A method of relating how much developed feature sizes differed from desired feature sizes was needed. The controlled parameters were the mask half-widths of both lines and contacts, the dose, and the n of the Mack development rate model. The following definitions were used:

L - length of a developed line at the resist-substrate interface.
W - half width of a developed line at the resist-substrate interface.
C - half of the width of a developed contact at the resist-substrate interface.

The measured outputs of the study were:
ΔL - difference between resist length L and ideal mask length.
ΔW - difference between resist half width W and ideal mask half width.
ΔC - difference between half width C and ideal mask half width.

Two Berkeley simulation programs were used to gather the necessary data. SPLAT 5.0 produced defocused aerial images of lines and contacts. A cutline of the image was then fed into SAMPLE 1.8b for resist exposure and subsequent development. The simulations were repeated with different mask sizes, doses, and development rate parameters. To help manage the accumulated data, the Berkeley simulation programs were interfaced to the TMA workbench, which had design of experiments and response surface analysis as helpful capabilities. What follows is a more detailed explanation of the simulation baselines and how the data was gathered and processed by TMA.

It was necessary to establish a baseline for the mask line length, mask line width, mask contact size, dose, and n parameter of the Mack model. Test cases were simulated with SPLAT and SAMPLE to select the values of unchanging parameters.

In SPLAT, symmetry was used in creating mask patterns. The pattern of the first quadrant of the 2-dimensional mask was mirrored across the x- and y-axes. This justified the use of half-width and half-contact size as input parameters. The mask line length in the first quadrant extended 1 um from the origin; the mask line width was set at 0.5 um; contact width was chosen to be 0.6 um. An i-line process was chosen with wavelength of 0.365 um and numerical aperture of 0.5. A defocus of 0.73 um was included in the imaging simulation.

The simulation of the resist development conducted by SAMPLE also required some specified values. The two-dimensional profiles generated by SAMPLE were sufficient in describing the development of the resist because image cutlines along the length *and* the width of the feature were simulated. The SPECTRALITH resist was chosen with A-B-C parameters of 0.574, 0.036, and 0.028 respectively. The baseline dose of 30 mJ/cm^2 was large enough to develop a 1 um thick photoresist layer with little line-end shortening after a 40 sec development time for the mask pattern described in the previous paragraph. A post-exposure bake of 0.04 um was incorporated into the simulation to reduce the standing-wave pattern in the developed resist. Choosing a resist development rate model was more involved.

The Kim, Hirai, and Mack development rate models were examined (again Figure 4). Initially the Kim model was of interest because of the possibility of modeling surface rate-retardation as a means of reducing top-loss. Furthermore, the Kim model served as a convenient starting point for a simulation of a depth-dependent rate *increase* model. A depth-dependent rate increase model was tested, but the model produced excessive undercutting of the photoresist line-end, so the model was dropped from consideration. The Hirai model was too sensitive to exposure (again Figure 4). The Mack model was finally chosen because it simulated better tolerance to low-intensity exposure than the Kim model. Furthermore, the threshold of development could be adjusted by varying the n-parameter of the model. The baseline values of the Mack model used in this study are listed in Table 1 above. The baseline values are restated in Tables 2 and 3 for convenience.

Table 2: SPLAT Baseline Parameters

SPLAT Parameter	Value
Wavelength	0.365 um
Numerical Aperture	0.50
Defocus	0.73 um
Mask line width	0.5 um
Mask Contact Size	0.6 um

Table 3: SAMPLE Baseline Parameter Values

SAMPLE Parameter	Value
A	0.574
B	0.036
C	0.028
Dose	30 mJ/cm^2
Heat Diffusion	0.04 um
Rmax	0.2284 um/sec
Rmin	0.0016 um/sec
a	0.005
n	5.6

The need to gather a large number of data points motivated the use of the TMA workbench. The workbench is a user interface that links different simulation programs to generate data for an experiment. Different commands are grouped into a module represented by an icon in the workbench interface. Opening the icon allows the user to select the values of different inputs.

SPLAT and SAMPLE were connected to the TMA workbench with Perl code. The Perl wrappers completed template files containing the skeletons of the SPLAT and SAMPLE commands with input parameter values. The values of the parameters were provided by the workbench interface. The workbench created a separate directory for each unique input set for SPLAT and SAMPLE programs. The directories contained distinct input files that were produced by merging the parameter values from the interface with the input template files for SPLAT and SAMPLE. Once the input files were generated, the workbench ran SPLAT and SAMPLE. A command in SPLAT (trial 14) took a specified cutline of relative image intensity and placed the information into a file named '2ddat'. SAMPLE incorporated the information of the file '2ddat' into the resist development simulation upon receiving the 'readimage' command.

The design of experiments (DOE) feature of the TMA workbench was particularly useful

in preparing different inputs for simulation. The mask half-size, dose, and n were mafked as control parameters that would form the design. A center composite inscribed (CCI) pattern was selected to distribute points for the three design parameters. The CCI pattern produced five equally spaced values for each design parameter. The design of experiments feature conveniently distributed fifteen data points over the specified range of the three controlled inputs, thus avoiding manual entry of each data point into the TMA interface. For this study, data points over a mask-half-line width range from 0.2 um to 0.4 um, a mask half hole-size range from 0.25 to 0.35 um, a dose range from 10 to 150 mJ/cm^2, and a n range from 3 to 8. To obtain more detailed information, the design of experiments was iterated using smaller subranges of inputs. For example, a set of data was generated by setting the dose range from 10 to 20 mJ/cm^2 while the n range was set at 4 to 5; then the dose range was incremented by 10 mJ/cm^2, and fifteen new points were obtained. The process was repeated until the total range of inputs had been tested with tightly focused patches CCI points.

The output files were automatically placed into their corresponding directories upon completion of the SPLAT or SAMPLE simulation. The TMA workbench examined the output files of the SAMPLE simulations and extracted the input parameters of mask half-feature size, dose, and n; differences between developed and ideal feature sizes; and wall angles into a table. The table values were copied into the workbench's spreadsheet, where underdeveloped and overdeveloped data were deleted. Underdeveloped or overdeveloped line-ends both had a ΔL of -1.000 um. Underdeveloped lines and contacts had W and C values that approached 0.000 um. Such points were removed from the spreadsheet. The valid data was then saved.

A note must be made about the interface between SPLAT and SAMPLE. Although the SAMPLE output files containing the developed profiles that were produced from a SPLAT generated image were of the correct length, SAMPLE's text output file made certain assumptions when writing the values of the 'distance to mask edge'. (The values of ΔL, W, and C were values of 'distance to mask-edge' in the SAMPLE output file.) SAMPLE assumed that the relative image intensity information was always 2 um wide. SAMPLE also assumed there was only one mask edge located at the center of the developed profile plot. Thus the cutline of relative image intensity from SPLAT had to be chosen to be 2 um wide.

For line-ends, the SAMPLE output file contained correct values of ΔL under 'distance to mask edge'; ΔW and ΔC were obtained with some additional processing. For the line width and contact cases, there were two mask edges. Recall that SAMPLE always assumed one mask edge at the center of the developed profile. The line width and contact images were specified in the interface such that the relative image intensities were 2 um wide with the feature centered at 1 um. The TMA workbench was configured to extract the absolute value of the final 'distance to mask edge' value in the SAMPLE output file. This value was actually half of the width of the developed feature. To obtain ΔW and ΔC, the mask half size was subtracted from the absolute value of the 'distance to mask edge'. This was accomplished by writing a short awk script to process the spreadsheet data for line widths and contact holes. The resulting file replaced the half-sizes with ΔW and ΔC. The corrected files were then loaded back into the TMA workbench's spreadsheet.

A response surface model was opened from the spreadsheet. The workbench was directed to generate a 6th degree polynomial model of each output parameter from the spreadsheet data. Each term of the polynomial had a factor no greater than 2nd degree for each control input. Once the model was constructed, the information was passed to the workbench's contour plotter. The response surface plots were examined to look for conditions that would be optimal over all three features. Dose latitudes were calculated from the plots, and resulting wall-angles were noted for each feature.

IV. Simulation Results

The goal of this study was to find a set of processing conditions that will optimize differences in line length, line width, and contact size from their ideal sizes. It was assumed that the different features were imaged on the same mask. The processing conditions that were studied were the mask width of the feature, the dose, and the contrast parameter of the Mack model, n. The data obtained from the SPLAT and SAMPLE simulations are shown as response surface plots for each feature. The following plots were made:

- Figure 5: ΔL as a function of Dose and n, mask line width = 0.5 um
- Figure 6: Wall-angle for Line-end as a function of Dose and n. mask line width = 0.5 um
- Figure 7: ΔW as a function of Dose and n, mask line width = 0.5 um
- Figure 8: Wall-angle for Line width as a function of Dose and n, mask line width = 0.5 um
- Figure 9: ΔC as a function of Dose and n, mask contact size = 0.6 um
- Figure 10: Wall-angle for Contact as a function of Dose and n, mask contact size = 0.6 um
- Figure 11: ΔC as a function of Contact Half size and n, dose = 30 um

Figure 5: ΔL (um), mask width = 0.5 um

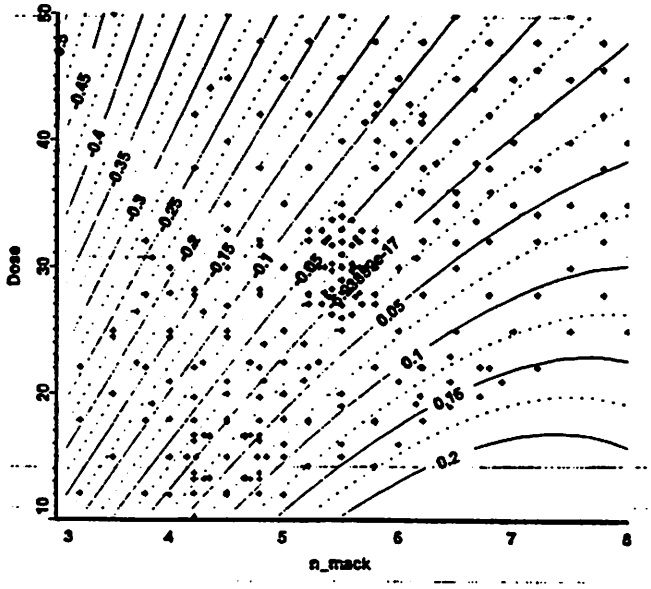

Figure 6: Wall angle for ΔL (deg), mask width = 0.5 um

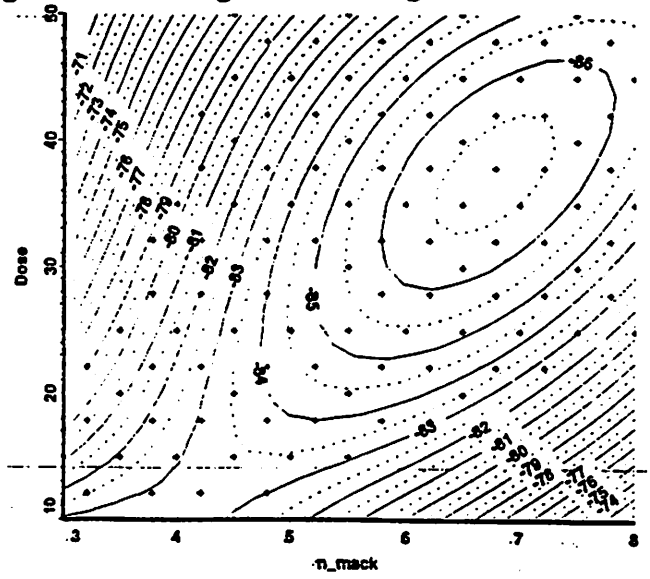

Figure 7: ΔW (um), mask width = 0.5 um

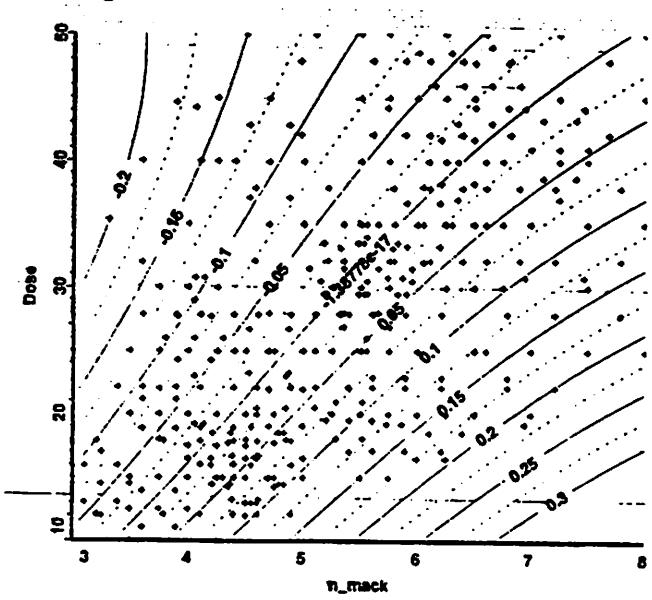

Figure 8: Wall angle for ΔW (deg), mask width = 0.5 um

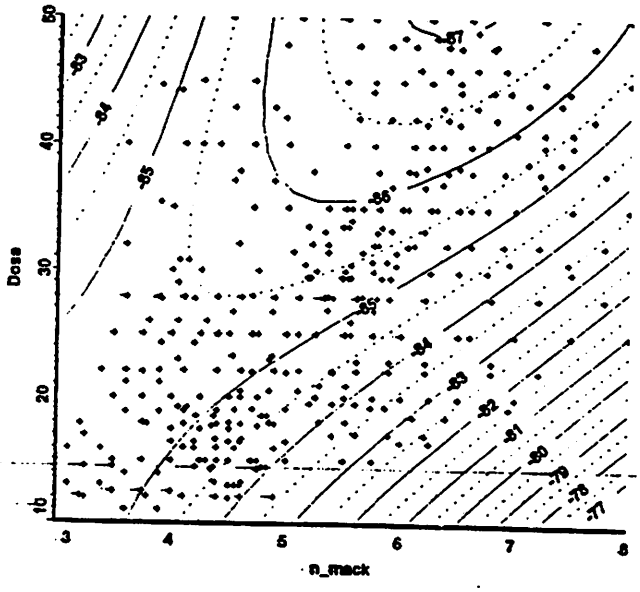

Figure 9: ΔC (um), mask width = 0.6 um

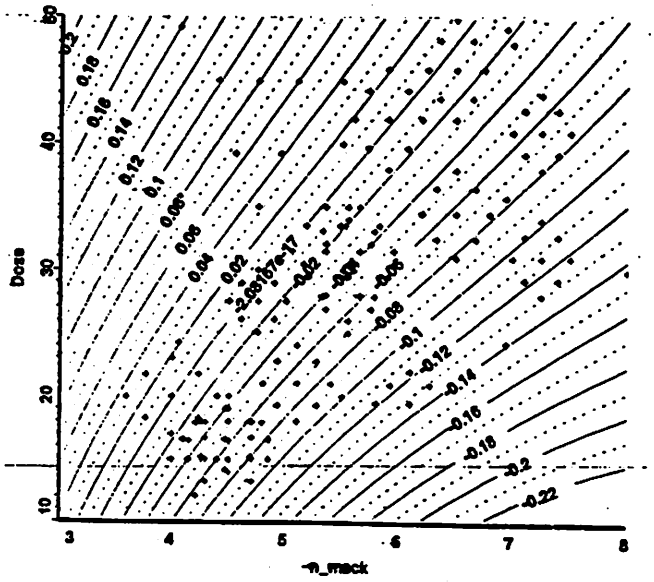

Figure 10: Wall angle for ΔC (deg), mask width = 0.6 um

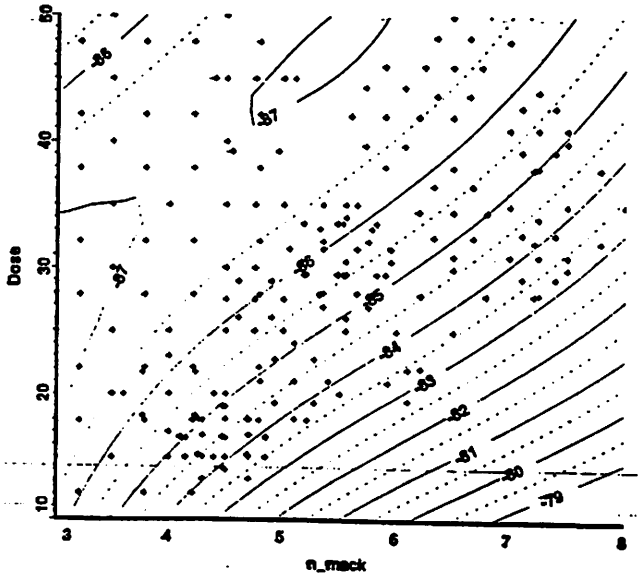

Figure 11: ΔC (um), dose = 30 mJ/cm^2

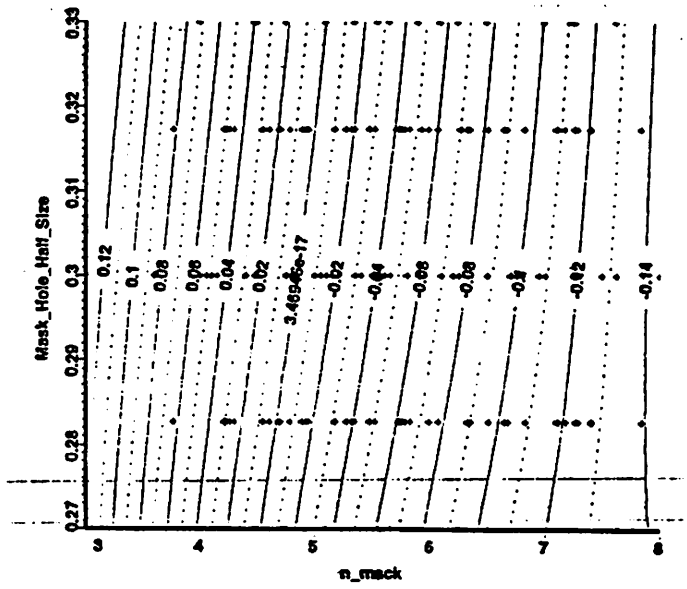

Examining these plots yielded information about the best processing conditions for each feature. The curves show ΔL, ΔW, and ΔC as a function of dose and n. Three values of n were chosen. For each n, the dose that produced zero deviation of the developed feature from the ideal mask was found. The doses that yielded a ten percent variation (5%) for L, W , and C were also obtained. A percent dose latitude was calculated by dividing the difference in maximum and minimum doses by the dose that produced zero deviation and multiplying by 100:

$$lattitude = 100 \times \frac{(dose_{max} - dose_{min})}{dose_{zero}}$$

The data has been summarized in Tables 4, 5, and 6.

Table 4: Processing Conditions for ΔL=0 um, mask line width=0.5 um

	Point 1	Point 2	Point 3	Unit
n	4.5	5.6	6.7	--
Dose	18.0	28.0	38.0	mJ/cm^2
Dose @ ΔL=+0.05	14.0	23.6	32.0	mJ/cm^2
Dose @ ΔL=-0.05	22.0	34.0	44.5	mJ/cm^2
Dose Latitude	44.4	37.1	32.9	%
Wall Angle	-83.5	-85.6	-86.6	°
ΔW	+0.030	+0.0375	+0.032	um
ΔC	-0.048	-0.055	-0.058	um

Table 5: Processing Conditions for ΔW=0 um, mask line width=0.5 um

	Point 1	Point 2	Point 3	Unit
n	4.5	5.6	6.7	--
Dose	21.3	32.8	42.6	mJ/cm^2
Dose @ ΔW=+.025	20.0	31.2	40.1	mJ/cm^2
Dose @ ΔW=-.025	22.8	34.6	44.4	mJ/cm^2
Dose Latitude	13.1	10.4	8.2	%
Wall Angle	-85.1	-85.7	-86.4	°
ΔL	-0.045	-0.040	-0.0375	um
ΔC	-0.025	-0.029	-0.033	um

Table 6: Processing Conditions for ΔC=0 um, mask contact size=0.6 um

	Point 1	Point 2	Point 3	Unit
n	4.5	5.6	6.7	--
Dose	26.0	38.8	51.3	mJ/cm^2
Dose @ ΔC=+.015	23.3	35.8	47.3	mJ/cm^2
Dose @ ΔC=-.015	28.7	41.6	54.8	mJ/cm^2
Dose Latitude	20.8	14.9	14.6	%
Wall Angle	-86.1	-86.6	-86.8	°
ΔL	-0.085	-0.080	-0.090	um
ΔW	-0.038	-0.037	-0.050	um

It should be noted for ΔL, ΔW, and ΔC, if dose was held constant, larger values of n produced longer and wider lines, but smaller contacts. Also, the dose latitude for all three features decreased for larger n. A third observation was, the wall angle for all three features was closer to perpendicular for larger n. These trends can be seen in Tables 4, 5, and 6.

Figure 11 shows the dependency of developed contact size on mask size and n for a dose of 30 mJ/cm^2. It can be seen that although larger mask sizes produce larger contacts, deviations of developed contacts from the mask size (twice ΔC) do not change dramatically with the mask; yet it is sometimes possible to adjust the mask size to obtain the desired contact size. At an n of 4.5, ΔC was always positive; but assuming that a 0.6 um contact was desired, it would be possible to choose a contact mask half size of 0.288 um to produce a ΔC of 0.012 to obtain the desired contact size. At an n of 5.6, a 0.6 um contact could still be produced if an oversized mask of half size 0.33 um were used (the resulting ΔC was -0.03 um). At an n of 6.7, it was not possible to produce a 0.6 um contact by changing the size of the mask within 10%. Thus for certain doses, it may be possible to adjust the mask size to obtain the desired feature size.

Table 4 contains information about three processing points from the response surface model that would produce zero line-end shortening. If the 5% size latitude was desired, none of the points for zero line-end shortening yielded desirable line widths or contact sizes. The lines were too wide, and the contacts were too small. Choosing processing conditions to bring ΔW to zero produced contacts that were too small (Table 5). Optimizing the contact size to achieve $\Delta C=0$ was beneficial to neither the line length nor the line width. Here the dimensions of the developed line were too small (Table 6).

Processing conditions that would bring ΔL, ΔW, and ΔC simultaneously to zero were not found. It was also not possible to choose points that would simultaneously be within the 5% feature size constraint for ΔL, ΔW, and ΔC. This can be seen from the dose ranges for corresponding n-values in Tables 4, 5, and 6; for example, the dose ranges for ΔL and ΔC do not overlap for corresponding n-values. Therefore the solution was to tolerate a smaller developed contact size while having ΔL and ΔW within the 5% feature size constraint. The values of the compromise points are summarized in Table 7. The processing point with n equal to 6.7 and dose equal to 42.6 mJ/cm^2 for line mask width of 0.5 um and contact mask size of 0.6 um produced a line closest to the ideal mask; but the contact was undersized by 0.068 um. The wall angles for all three features were closest to perpendicular at an n of 6.7. It is useful to note that if a contact of 0.5 um had been desired, the 0.6 um mask size would have produced a contact that was only 0.032 um too large.

Table 7: Resulting ΔL, ΔW, and ΔC of Compromise Processing Points

	Point 1	Point 2	Point 3	Unit
n	4.5	5.6	6.7	--
Dose	21.0	32.6	42.6	mJ/cm^2
ΔL	-0.0375	-0.035	-0.0375	um
Wall Angle	-83.5	-85.7	-86.3	°
ΔW	+0.005	+0.005	+0.00	um
Wall Angle	-85.1	-85.7	-86.4	°
ΔC	-0.031	-0.029	-0.034	um
Wall Angle	-85.3	-85.9	-86.2	°

The simulations of the developed features provided information about the contributions of mask size, dose, and resist n-value to desired feature size. It was found that larger n required larger doses for accurate feature development but produced steeper wall angles. Although optimization of one feature type was possible, if all three feature sizes were to be optimized simultaneously, the plots generated from the response surface models were useful in finding the compromise processing conditions.

V. Summary

This work provided information about the effects of mask and resist on the development of lines and contacts. The SPLAT 5.0 and SAMPLE 1.8b simulators were linked with the TMA workbench to obtain the necessary data. The simulation results indicated that if the fabrication engineer was able to tolerate a 0.53 um contact from a 0.6 um ideal contact mask, line length and width could be brought within 5% tolerances by choosing a resist with n of 6.7 and dose of 42.6 mJ/cm^2. The TMA workbench provided the response surface modeling capabilities necessary to examine a large set of cases.

There were some possibilities for improvement in the simulators. Because SAMPLE 1.8b assumed only one mask edge located at the image pattern's center, an external script was needed to obtain ΔW and ΔC. An improvement to SAMPLE 1.8b would be a means of specifying where the mask edges are located with respect to the developed profile. This would require an update to the routines that generate the 'distance to mask edge' values to accommodate mask patterns of line widths and contacts. Furthermore, the above routine should be changed to function correctly for loaded image cutlines of lengths other than 2 um.

The TMA workbench was helpful in organizing the data for each feature, but if the capability to draw several response surface models on the same plot were added, the comparisons of lines and contacts in this work would have been easier to perform. Although the RSM plotter could overlay multiple contours generated from the same input values, an easy way to overlay contours generated from different input values was not found. This precluded an on-line comparison of ΔL, ΔW, and ΔC.

Nevertheless, the simulation and response surface modeling of these processing conditions provided a useful means of graphically representing the effect of mask and resist upon the development of lines and contacts. This increase of n from 5.6 and 6.7 indicates that the s-shaped resist dissolution rate curve is essential and that increasing this effect further in resist materials would be beneficial.

REFERENCES

[1] TMA WorkBench, product of Technology Modeling Associates made available for this project, *TMA WorkBench: IC Technology Design Environment Version 2.1 User's Manual*, Technology Modeling Associates, Inc., Sunnyvale, CA, August 1996.

[2] D. Lee, D. Newmark, K. Toh, P. Flanner, and A. R. Neureuther, *SPLAT v5.0 Users' Guide*, Electronics Research Laboratory, College of Engineering, University of California, Berkeley, CA, 1 March 1995.

[3] *SAMPLE 1.8a User's Guide*, Department of Electrical Engineering and Computer Sciences, University of California, Berkeley, CA, p.55, 1991

[4] S. H. Thornton. and C.A. Mack, "Lithography Model Tuning: Matching Simulation to Experiment," *SPIE Proceedings - Optical Microlithography IX*, vol. 2726, pp. 223-235, 13 - 15 March 1996.

[5] D. Kim, W. Oldham, and A. Neureuther, "Development of Positive Photoresist," *IEEE Transactions on Electron Devices*, vol. ED-31, pp. 1730-1735, December 1984

[6] Y. Hirai, M. Sasago, M. Endo, K. Tsuji, and Y. Mano, "Process Modeling for Photoresist Development and Design of DLR/sd (Double-Layer Resist by a Single Development) Process," *IEEE Transactions on Computer-Aided Design*, vol. CAD-6, No. 3, pp. 403-409, May 1987.

[7] S. H. Thornton. and C.A. Mack, "Lithography Model Tuning: Matching Simulation to Experiment," *SPIE Proceedings - Optical Microlithography IX*, vol. 2726, pp. 223-235, 13 - 15 March 1996.